Intelligent Control of Wind Conversion System based on PMSG using T-S Fuzzy Scheme

Naziha Harrabi*‡, Mansour Souissi*, Abdel Aitouche**, Mohamed Chaabane*

*Lab-STA, National Engineering School of Sfax, 3072, Tunisia.

** CRIStAL Laboratory, Hautes Etudes d'Ingenieur, Lille, France.

(nozha.harrabi@gmail.com, Mansour.souissi@ipeis.rnu.tn, abdel.aitouche@hei.fr, chaabane@enis.rnu.tn)

‡ Corresponding Author; N. Harrabi; email: nozha.harrabi@gmail.com.

Received: 09.06.2015 Accepted:21.07.2015

Abstract- This paper presents a topology of control dedicated to a wind energy conversion system (WECS) using a Permanent Magnet Synchronous Generator (PMSG) and AC/DC rectifier in the objective of ensuring maximum power generation. The control aim is to track the generator reference speed according to the wind velocity variation in order to maximize the power output and enhance system performance. For this purpose, the WECS modelling is carried out on the basis of Takagi–Sugeno (T-S) fuzzy model. The control gains are calculated by solving Linear Matrix Inequalities (LMIs). Finally, simulation results have been presented to check the proposed approach efficiency.

Keywords—Wind energy conversion system, PMSG, AC/DC converter, T-S fuzzy control, linear matrix inequality (LMI).

1. Introduction

The global warming effect together with the diminishing reserves of fossil fuels has contributed to increasing attention given to renewable electrical energy. By all of different forms of renewable energy, the wind energy has been recognized as the main source in power industry. The wind power resources are massive among the world. It has been evaluated that only 10% of raw wind potential are able to satisfy all the world requirements in electricity if it could be put to use [1]. In light of this, improving the performance of wind turbines and wind energy conversion systems (WECS) is progressively increasing attention as a topic research.

Because of the increase of the turbine power range, it has been needed to establish an interface which provides connection between the wind turbine and the grid. As a solution, power electronics are already introduced to make the link, then different topologies for power conversion schemes are adopted in literature. Many generator-converter systems have been popularly used such as in [2, 3, 22, 23]. The most widespread topology in industry is the six pulse diode rectifier and pulse width modulated (PWM) inverter because of its low cost as in [25] ,whereas, this technology allows the power flow in only one direction contrarily to back-to-back power converter. The latter permits the bidirectional power flow which is interesting in certain applications.

Many researchers have proposed various control schemes in order to extract the optimal accessible power given by the WECS [4]. The simplest techniques for searching the maximum power point are based on PI controller and Perturb and Observe algorithm [5, 6], but these methods are still classical and lack of performance. Another known method is neural network method which estimates the wind velocity from the measured wind power and generator speed, and consequently the maximum power generator speed control or torque reference can be deduced for the operational point tracker [7,8]. Even though neural network may guarantee fast response, the performance of control fails along the system variation. Furthermore, fuzzy logic methods have been widely adopted and they have presented better effectiveness [9, 10, 26]. However, the major problems of most of these methods are lack of stability and strict theoretical analysis so that the maximum power point varies over a wide range. In order to overcome this problem, sliding mode control is applied in several works [11, 12], but its main drawback is its complexity and the difficulty of implementation.

In comparison, Takagi-Sugeno (T-S) modelling has proved its performance in the study of nonlinear systems. In that sense, the control based on (T-S) model has been more popular as one of the most successful techniques for systems and control applications due to its reliability and effectiveness. Considerable researches are investigated e.g. [13, 14, 15, 21].

The principal benefit of T-S fuzzy approach is that it provides a simple way to construct the controller since it is systematically constructed based on Parallel Distributed Compensation (PDC) together with Linear Matrix Inequality (LMI) method [14]. The fuzzy model of Takagi Sugeno allows modelling the nonlinear system by representing local dynamics by linear models. Therefore, the global system model is achieved by a combination of the different linear models. Then, a linear feedback control has to be constructed for every local linear model. Accordingly, the consequent overall nonlinear controller is once more a fuzzy combination of each distinct linear controller [15]. The theory of Lyapunov stability is applied to realize the fuzzy controller. In other words, the stability analysis problem and the control design are reduced to LMI conditions which can be easily solved by using Matlab LMI toolbox [17].

During this paper, a description of the wind turbine modelling and control strategy is detailed. The topology of PWM rectifier-inverter that integrates PWM converters in the machine side and the grid side is investigated to offer the possibility of the bidirectional power flow.

The rest of this paper is arranged as following: in the second section, a dynamic modelling of the WECS is presented. The third section starts with presenting the control strategy. Then, fuzzy modelling of the system is presented. Finally, the control design is explained and stability conditions are given. Section 4 is reserved to present numerical simulations that illustrate the effectiveness of the proposed control topology. We finish by conclusions in the last section.

2. Wind Energy Conversion System Modelling

During this section, the electrical and mechanical modeling of the WECS is detailed. A schematic overview of the WECS is shown in Fig.1. The conversion chain consists of a fixed-pitch turbine that captures the wind energy coupled with a PMSG which permits the transformation of the mechanical captured power to electrical power. Power electronic converters are employed in association with PMSG in order to maintain the power at its optimum with various wind speed.

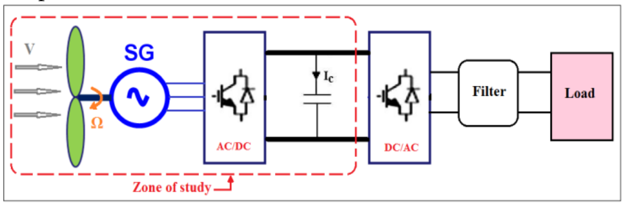

Fig. 1. Structural diagram of the wind energy conversion system

The work treated in the current paper focuses only in the mentioned wind conversion subsystem.

2.1. Wind turbine characteristics

The aerodynamic power produced by the wind turbine is described by the following equation [24]:

$$P_t = 0.5C_p(\lambda,\beta)\rho A v^3 \tag{1}$$

Where A is the swept area of the wind turbine (m^2), ρ is the air density ($Kg.m^{-3}$), v is the wind velocity ($m.s^{-1}$), and $C_p(\lambda)$ is the power coefficient which is depending on the pitch angle β and the tip-speed ratio λ given by [24]:

$$\lambda = \frac{R\Omega}{v} \tag{2}$$

where R is the blade length and Ω represents the wind turbine rotational speed.

The maximum C_p value is obtained for β = 0º and a specific value of λ which corresponds to the optimal speed ratio value (λ_{opt}). Thus, when assuming both $C_{p(max)}$ and λ_{opt} are known, the maximum power generated by the wind turbine satisfies:

$$P_{t(\max)} = 0.5C_{p(\max)}(\lambda_{opt})\rho\pi R^5\Omega_r^3 / \lambda_{opt}^3 \tag{3}$$

The mechanical torque given by the turbine rotor is expressed by the following relationship:

$$T_m = P_{t(\max)} / \Omega = 0.5C_{p(\max)}(\lambda_{opt})\rho\pi R^5\Omega_r^2 / \lambda_{opt}^3 \tag{4}$$

The maximum wind energy conversion occurs at the maximum power coefficient $C_{p(max)}$ by changing the rotor speed to maintain the speed ratio at its optimum λ_{opt}, T_m is then given by:

$$T_{m(ref)} = K_o\, \Omega_r^{\,2} \tag{5}$$

where $K_o=0.5C_{p(max)}\,\rho\pi R^5/\lambda_{opt}^3$

The expression of electromagnetic torque in the rotor in d-q reference frame is given by:

$$T_{em} = p[(L_{sq} - L_{sd})i_{sd}i_{sq} + \Psi_f i_{sq}] \tag{6}$$

where p being the number of pole pairs, ψ_f is the magnetic flux, i_{sd} and i_{sq} are the stator current (d,q) components. L_{sd} is the direct axis inductance, L_{sq} is the inductance in quadrature.

For smooth poles $L_{sd} = L_{sq} = L_s$, so that (6) becomes:

$$T_{em} = p\Psi_f i_{sq} \tag{7}$$

The PMSG mechanical speed evolution is determined using the following relationship:

$$J\frac{d\Omega}{dt} = T_m - T_{em} - f\Omega \tag{8}$$

where J and f denote respectively the moment of inertia of the PMSG and the friction coefficient.

2.2. The generator and rectifier modelling

Generally, the voltage produced by the voltage source converter can be expressed by defining switching functions for each phase of the converter. These switches are complementary; their role is to establish a connection between the AC side and the DC bus.

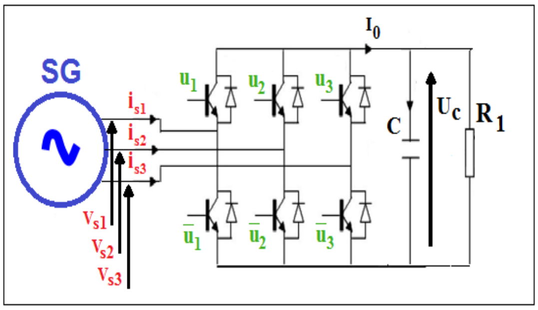

Fig. 2. Synchronous generator associated to the rectifier

The input three phases voltages V_{si} (i=1,2,3) and the output current I_0 can be written in function of β_i which denotes the average value of u_i over the PWM period, the output DC side voltage U_c, and the input currents i_{si}:

$$\begin{bmatrix} V_{s1} \\ V_{s2} \\ V_{s3} \end{bmatrix} = \frac{1}{6}\begin{bmatrix} 2\beta_1 & -\beta_2 & -\beta_3 \\ -\beta_1 & 2\beta_2 & -\beta_3 \\ -\beta_1 & -\beta_2 & \beta_3 \end{bmatrix} U_c \tag{9}$$

$$I_0 = \frac{1}{2}\begin{bmatrix} (1+\beta_3) & (1+\beta_3) & (1+\beta_3) \end{bmatrix}\begin{bmatrix} i_{s1} \\ i_{s2} \\ i_{s3} \end{bmatrix} \tag{10}$$

Since the stator three-phase currents:

$$i_{s1} + i_{s2} + i_{s3} = 0$$

we obtain:

$$I_0 = \frac{1}{2}\begin{bmatrix} \beta_1 & \beta_2 & \beta_3 \end{bmatrix}\begin{bmatrix} i_{s1} \\ i_{s2} \\ i_{s3} \end{bmatrix} \tag{11}$$

The average voltage at the rectifier output verifies the following equation:

$$\frac{dU_c}{dt} = \frac{1}{2C}\begin{bmatrix} \beta_1 & \beta_2 & \beta_3 \end{bmatrix}\begin{bmatrix} i_{s1} \\ i_{s2} \\ i_{s3} \end{bmatrix} - \frac{U_C}{R_1 C} \tag{12}$$

Using the d-q reference frame, the above equations can be written as:

$$\begin{bmatrix} v_{sd} \\ v_{sq} \end{bmatrix} = \frac{1}{2}\begin{bmatrix} \beta_d \\ \beta_q \end{bmatrix} U_c \tag{13}$$

$$I_0 = \frac{3}{4}\begin{bmatrix} \beta_d & \beta_q \end{bmatrix}\begin{bmatrix} i_{sd} \\ i_{sq} \end{bmatrix} \tag{14}$$

$$\frac{dU_c}{dt} = \frac{3}{4C}\begin{bmatrix} \beta_d & \beta_q \end{bmatrix}\begin{bmatrix} i_{sd} \\ i_{sq} \end{bmatrix} - \frac{U_C}{R_1 C} \tag{15}$$

The stator current in d-q reference frame is given by:

$$\begin{bmatrix} \frac{d}{dt} i_{sd} \\ \frac{d}{dt} i_{sq} \end{bmatrix} = \begin{bmatrix} -\frac{R_S}{L_S} & w \\ -w & -\frac{R_S}{L_S} \end{bmatrix}\begin{bmatrix} i_{sd} \\ i_{sq} \end{bmatrix} + \begin{bmatrix} \frac{1}{L_S} & 0 \\ 0 & \frac{1}{L_S} \end{bmatrix}\begin{bmatrix} E_d \\ E_q \end{bmatrix} - \frac{1}{2L_S}\begin{bmatrix} \beta_d \\ \beta_q \end{bmatrix} U_c \tag{16}$$

Where w=pΩ is the electrical angular speed, R_s and L_s denote respectively the synchronous resistance and inductance, E_d and E_q are the electromotive force (d,q) components given by:

$$E_d = 0 \qquad E_q = p\psi_f \Omega$$

The voltage dynamic equations of the stator in the d − q reference frame can be stated as :

$$\begin{cases} v_{sd} = -R_s i_{sd} - L_s \dfrac{di_{sd}}{dt} + p\Omega L_s i_{sq} = \dfrac{U_c}{2}\beta_d \\ v_{sq} = -R_s i_{sq} - L_s \dfrac{di_{sq}}{dt} - p\Omega L_s i_{sd} + p\Omega \Psi_f = \dfrac{U_C}{2}\beta_q \end{cases} \tag{17}$$

3. Maximum Peak Power Tracking Algorithm

3.1. The control strategy principle

The following figure summarizes the control scheme treated in the current work in the aim to maintain generated power at its maximum value.

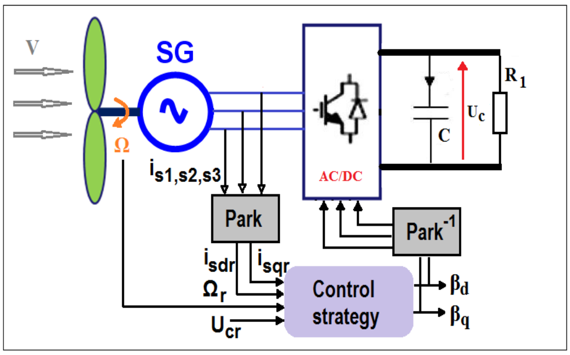

Fig. 3. Control strategy of the WECS

Since the optimum energy conversion is obtained at λ_{opt}, the constraint $\lambda = \lambda_{opt}$ implies that the mechanical rotor speed have to vary in proportion with the wind velocity to be particular; $\Omega_r = \frac{\lambda_{opt} V_v}{R}$ .Thus, the turbine can be controlled to produce maximum power given by (3) as wind speed fluctuates.

Once the rotor speed reference is determined, we can calculate the reference of the current in quadrature given by:

$$i_{sqr} = -\frac{K_o}{p\psi_f}\Omega_r^2 \tag{18}$$

For this study, we suppose that the direct current reference $i_{sdr} = 0$.

Using the relationship between bus voltage and stator current in q-axis described in (17), the bus voltage reference can be determined by the following expression:

$$U_{cr} = \frac{2}{\beta_q}(p\psi_f \Omega_r) \tag{19}$$

3.2. TS Fuzzy model of wind energy conversion system

Due to the nonlinearity of the WECS, T-S modeling permits to represent its behavior by the introduction of a set of linear submodels. Each sub-model leads to the overall behavior of the nonlinear system using a weighting function. Introducing the state vector:

$x(t) = [i_{sd} \quad i_{sq} \quad U_c \quad \Omega]^T$,

and the input signal:

$u(t) = [\beta_d \quad \beta_q]^T$,

the average model of the WECS can be described by the following equations:

$$\begin{bmatrix} \frac{d}{dt} i_{sd} \\ \frac{d}{dt} i_{sq} \\ \frac{d}{dt} U_c \\ \frac{d}{dt} \Omega \end{bmatrix} = \begin{bmatrix} \frac{-R_s}{L_s} & p\Omega & 0 & 0 \\ -p\Omega & \frac{-R_s}{L_s} & 0 & \frac{p\psi_f}{L_s} \\ \frac{3}{4C}\beta_d & \frac{3}{4C}\beta_q & -\frac{1}{R_1 C} & 0 \\ 0 & -\frac{p\psi_f}{J} & 0 & \frac{K_o\Omega - f}{J} \end{bmatrix} \begin{bmatrix} i_{sd} \\ i_{sq} \\ U_c \\ \Omega \end{bmatrix} + \begin{bmatrix} \frac{-U_c}{2L_s} & 0 \\ 0 & \frac{-U_c}{2L_s} \\ 0 & 0 \\ 0 & 0 \end{bmatrix} \begin{bmatrix} \beta_d \\ \beta_q \end{bmatrix} \tag{20}$$

$$\dot{x}(t) = A(x,u)x(t) + B(x)u(t) \tag{21}$$

$$y(t) = Cx(t) \tag{22}$$

With $C = \begin{bmatrix} 1 & 0 & 0 & 0 \\ 0 & 1 & 0 & 0 \\ 0 & 0 & 1 & 0 \\ 0 & 0 & 0 & 1 \end{bmatrix}$

Considering the fuzzy premise variables $q_j(t)$

$$q_1(t) = \Omega; q_2(t) = \beta_d; q_3(t) = \beta_q; q_4(t) = U_c \tag{23}$$

thus, system (20) is easily described by T-S fuzzy rules as follows:

If $q_1(t)$ is S_{1i} and …and $q_4(t)$ is S_{4i}, then

$$\dot{x}(t) = A_i x(t) + B_i u(t) \tag{24}$$

$$y(t) = Cx(t) \tag{25}$$

S_{ji} denotes the fuzzy sets, r represents the fuzzy rules number (r=16) and A_i and B_i are the local subsystem matrices given by:

$$A_i = \begin{bmatrix} \frac{-R_s}{L_s} & pq_{1i} & 0 & 0 \\ -pq_{1i} & \frac{-R_s}{L_s} & 0 & \frac{p\psi_f}{L_s} \\ \frac{3}{4C}q_{2i} & \frac{3}{4C}q_{3i} & -\frac{1}{R_1 C} & 0 \\ 0 & -\frac{p\psi_f}{J} & 0 & \frac{K_o q_{1i} - f}{J} \end{bmatrix}$$

$$B_i = \begin{bmatrix} \frac{-q_{4i}}{2L_s} & 0 \\ 0 & \frac{-q_{4i}}{2L_s} \\ 0 & 0 \\ 0 & 0 \end{bmatrix}$$

The response of a TS model is a weighted sum stated as follows:

$$\begin{cases} \dot{x}(t) = \sum_{i=1}^{r} \mu_i(q(t))\{A_i x(t) + B_i u(t)\} \\ y(t) = Cx(t) \end{cases} \quad (26)$$

Where the vector q(t) is defined as:

$$q(t) = \begin{bmatrix} q_1(t) \\ q_2(t) \\ q_3(t) \\ q_4(t) \end{bmatrix}$$

The degree of activation for rule i is normalized as:

$$\mu_i(q(t)) = \frac{w_i(q(t))}{\sum_{i=1}^{r} w_i(q(t))} \quad (27)$$

with $w_i(q(t)) = \prod_{j=1}^{4} S_{ji}(q(t))$. (28)

These weighting functions verify the following properties:

$$\begin{cases} \sum_{i=1}^{r} \mu_i(q(t)) = 1 \\ 0 \le \mu_i(q(t)) \le 1 \end{cases} \quad \text{for all t.} \quad (29)$$

The membership functions are written in the general form as:

$$f_j = \frac{q_j(t) - m_j}{M_j - m_j} \quad (30)$$

$$\bar{f}_j = 1 - f_j \quad (31)$$

Where M_j and m_j are respectively the maximum and the minimum bounds of the variable $q_j(t)$ for j=1,2,3,4 .

The following table presents the setting of the parameters q_{ji} setting according to each rule for i=1..16.

Table 1. Fuzzy controller rules

Rule index i	Fuzzy Sets of rules				Parameters of then-part			
	s_{1i}	s_{2i}	s_{3i}	s_{4i}	q_{1i}	q_{1i}	q_{1i}	q_{1i}
1	f_1	f_2	f_3	f_4	M_1	M_2	M_3	M_4
2	f_1	f_2	f_3	$\bar{f}_4$	M_1	M_2	M_3	m_4
3	f_1	f_2	$\bar{f}_3$	f_4	M_1	M_2	m_3	M_4
4	f_1	$\bar{f}_2$	$\bar{f}_3$	$\bar{f}_4$	M_1	M_2	m_3	m_4
5	f_1	$\bar{f}_2$	f_3	f_4	M_1	m_2	M_3	M_4
6	f_1	$\bar{f}_2$	f_3	$\bar{f}_4$	M_1	m_2	M_3	m_4
7	f_1	$\bar{f}_2$	$\bar{f}_3$	f_4	M_1	m_2	m_3	M_4
8	f_1	$\bar{f}_2$	$\bar{f}_3$	$\bar{f}_4$	M_1	m_2	m_3	m_4
9	$\bar{f}_1$	f_2	f_3	f_4	m_1	M_2	M_3	M_4
10	$\bar{f}_1$	f_2	f_3	$\bar{f}_4$	m_1	M_2	M_3	m_4
11	$\bar{f}_1$	f_2	$\bar{f}_3$	f_4	m_1	M_2	m_3	M_4
12	$\bar{f}_1$	f_2	$\bar{f}_3$	$\bar{f}_4$	m_1	M_2	m_3	m_4
13	$\bar{f}_1$	$\bar{f}_2$	f_3	f_4	m_1	m_2	M_3	M_4
14	$\bar{f}_1$	$\bar{f}_2$	f_3	$\bar{f}_4$	m_1	m_2	M_3	m_4
15	$\bar{f}_1$	$\bar{f}_2$	$\bar{f}_3$	f_4	m_1	m_2	m_3	M_4
16	$\bar{f}_1$	$\bar{f}_2$	$\bar{f}_3$	$\bar{f}_4$	m_1	m_2	m_3	m_4

3.3. *Error state model*

In order to ensure a smooth tracking of the references, we introduce a state reference vector: $x_r(t) = [i_{sdr} \quad i_{sqr} \quad U_{cr} \quad \Omega_r]^T$. Defining $e(t) = x(t) - x_r(t)$ as the state tracking errors, hence the new PDC fuzzy controller is designed such as:

$$u(t) = -\sum_{i=1}^{r} \mu_i(q(t)) K_i e(t) \quad (32)$$

Thus, we can describe the resulting dynamic error model as follows:

$$\dot{e}(t) = \sum_{i=1}^{r} \mu_i(q(t))(A_i(t) + B_i u(t) + A_i x_r) \quad (33)$$

Another state variable $e_I = \int e$ corresponding to an integral action on the tracking error is employed in the PDC fuzzy controller so as to avoid steady state errors, then the control law is written as:

$$u(t) = -\sum_{i=1}^{r} \mu_i(q(t)) \begin{bmatrix} K_i & F_i \end{bmatrix} \begin{bmatrix} e(t) \\ e_I(t) \end{bmatrix}$$

$$= -\sum_{i=1}^{r} \mu_i(q(t)) \bar{K}_i \bar{e}(t) \tag{34}$$

Where $\bar{K}_i = \begin{bmatrix} K_i & F_i \end{bmatrix}$ and $\bar{e}(t) = \begin{bmatrix} e(t) & e_I(t) \end{bmatrix}^T$.

Therefore, we can write the T-S model in the augmented form as follows:

$$\dot{\bar{e}}(t) = \sum_{i=1}^{r} \mu_i(q(t))[\bar{G}_i \bar{e}(t) + \bar{D}_i \bar{h}] \tag{35}$$

With:

$$\bar{G}_i = \bar{A}_i - \bar{B}_i \bar{K}_i \qquad \bar{A}_i = \begin{bmatrix} A_i & 0 \\ I & 0 \end{bmatrix} \qquad \bar{B}_i = \begin{bmatrix} B_i \\ 0 \end{bmatrix}$$

$$\bar{D}_i = \begin{bmatrix} A_i & 0 \\ 0 & 0 \end{bmatrix} \qquad \bar{h} = \begin{bmatrix} x_r \\ 0 \end{bmatrix}$$

3.4. LMI formulation for H_∞ performance

In order to ensure smooth reference tracking under the influence of perturbation, the H_∞ tracking performance which has been considered in several works [18], [19] and [20], is adopted.

$$\int_0^\infty \bar{e}^T(t)\bar{e}(t)dt < \gamma^2 \int_0^\infty \bar{h}^T \bar{h} dt \tag{36}$$

Where γ is a defined value.

In the aim of analyzing the maximum power point tracking convergence, we consider the Lyapunov function candidate $V(\bar{e}) = \bar{e}^T P \bar{e}$ where $P = P^T > 0$ the common definite positive matrix. The Lyapunov function time derivative along the control dynamics has to satisfy:

$$\dot{V}(\bar{e}(t)) = \dot{\bar{e}}^T P \bar{e} + \bar{e}^T P \dot{\bar{e}} < 0 \tag{37}$$

The condition leading to accomplish the H-infinity performance associated to the tracking error is given as:

$$\dot{V}(\bar{e}(t)) + \bar{e}^T(t)\bar{e}(t) - \gamma^2 \bar{h}^T \bar{h} < 0 \tag{38}$$

By remplacing (37) and (35) in (38) we get:

$$\sum_{i=1}^{r} \mu_i(q(t)) \begin{Bmatrix} \bar{e}^T(t)[\bar{G}_i^T P + P_i \bar{G}_i^T]\bar{e}(t) \\ +\bar{h}^T[\bar{D}_i^T P]\bar{e}(t) \\ +\bar{e}^T(t)[P\bar{D}_i]\bar{h} \end{Bmatrix} - \gamma^2 \bar{h}^T \bar{h} < 0 \tag{39}$$

$$\begin{bmatrix} \bar{e}^T(t) & \bar{h}^T \end{bmatrix} \begin{bmatrix} \sum_{i=1}^{r} \mu_i(q(t))[\bar{G}_i^T P + P_i \bar{G}_i^T] + I & P\sum_{i=1}^{r} \mu_i(q(t))\bar{D}_i \\ \sum_{i=1}^{r} \mu_i(q(t))\bar{D}_i^T P & -\gamma^2 I \end{bmatrix} \begin{bmatrix} \bar{e}(t) \\ \bar{h} \end{bmatrix} < 0 \tag{40}$$

To check this inequality, it suffices to check that:

$$\begin{bmatrix} \sum_{i=1}^{r} \mu_i(q(t))[\bar{G}_i^T P + P_i \bar{G}_i^T] + I & P\sum_{i=1}^{r} \mu_i(q(t))\bar{D}_i \\ \sum_{i=1}^{r} \mu_i(q(t))\bar{D}_i^T P & -\gamma^2 I \end{bmatrix} < 0 \tag{41}$$

$$\begin{bmatrix} \sum_{i=1}^{r} \mu_i(q(t))[\bar{G}_i^T P + P_i \bar{G}_i^T] & P\sum_{i=1}^{r} \mu_i(q(t))\bar{D}_i \\ \sum_{i=1}^{r} \mu_i(q(t))\bar{D}_i^T P & -\gamma^2 I \end{bmatrix} + \begin{bmatrix} I & 0 \\ 0 & 0 \end{bmatrix} < 0 \tag{42}$$

$$\begin{bmatrix} \sum_{i=1}^{r} \mu_i(q(t))[\bar{G}_i^T P + P_i \bar{G}_i^T] & P\sum_{i=1}^{r} \mu_i(q(t))\bar{D}_i \\ \sum_{i=1}^{r} \mu_i(q(t))\bar{D}_i^T P & -\gamma^2 I \end{bmatrix} + \begin{bmatrix} I \\ 0 \end{bmatrix} \begin{bmatrix} I & 0 \end{bmatrix} < 0 \tag{43}$$

The use of Shur lemma allows writing:

$$\begin{bmatrix} \sum_{i=1}^{r} \mu_i(q(t))[\bar{G}_i^T P + P_i \bar{G}_i^T] & P\sum_{i=1}^{r} \mu_i(q(t))\bar{D}_i & I \\ \sum_{i=1}^{r} \mu_i(q(t))\bar{D}_i^T P & -\gamma^2 I & 0 \\ I & 0 & -I \end{bmatrix} < 0 \tag{44}$$

That means:

$$\begin{bmatrix} [\bar{G}_i^T P + P_i \bar{G}_i^T] & P\bar{D}_i & I \\ \bar{D}_i^T P & -\gamma^2 I & 0 \\ I & 0 & -I \end{bmatrix} < 0 \quad (45)$$

$$\begin{bmatrix} P^{-1} & 0 & 0 \\ 0 & I & 0 \\ 0 & 0 & I \end{bmatrix} \begin{bmatrix} [\bar{G}_i^T P + P_i \bar{G}_i^T] & P\bar{D}_i & I \\ \bar{D}_i^T P & -\gamma^2 I & 0 \\ I & 0 & -I \end{bmatrix} \begin{bmatrix} P^{-1} & 0 & 0 \\ 0 & I & 0 \\ 0 & 0 & I \end{bmatrix} < 0 \quad (46)$$

$$\begin{bmatrix} P^{-1}[\bar{G}_i^T P + P_i \bar{G}_i^T] P^{-1} & P^{-1} P\bar{D}_i & P^{-1} \\ \bar{D}_i^T P P^{-1} & -\gamma^2 I & 0 \\ P^{-1} & 0 & -I \end{bmatrix} < 0 \quad (47)$$

By choosing $X = P^{-1}$ and $M_i = \bar{K}_i P^{-1}$ and by using the T-S fuzzy control law, the maximum power generation of the WECS is accomplished if the controller gains are prescribed as $\bar{K}_i = M_i X^{-1}$ with the matrices X and M_i satisfying the following LMI:

$$\begin{bmatrix} \bar{A}_i^T X + X\bar{A}_i^T - \bar{B}_i M_i - M_i^T \bar{B}_i^T & \bar{D}_i & X \\ \bar{D}_i^T & -\gamma^2 I & 0 \\ X & 0 & -I \end{bmatrix} < 0 \quad (48)$$

4. Numerical Simulation

Matlab/Simulink is used for the simulation of the WECS. The numerical illustration considers the wind conversion system with the parameter values given by the following table:

Table 2. Wind conversion system parameters

Rated voltage	90V
Rated current	*4.8 A*
Rated power	*600 W*
Number of poles	*8*
Synchronous resistance	*1.13 Ω*
Synchronous inductance	*1 mH*
Friction coefficient	*0.006 N.m.s/rad*
Moment of inertia	*0.005 N.m*
Blade length	*0.5 m*
Air density	*1.2 Kg/**m²***
Magnetic flux	*0.16 wb*

The proposed strategy of control is tested for different wind velocity variations. The wind speed signal variation is presented in Fig.4.

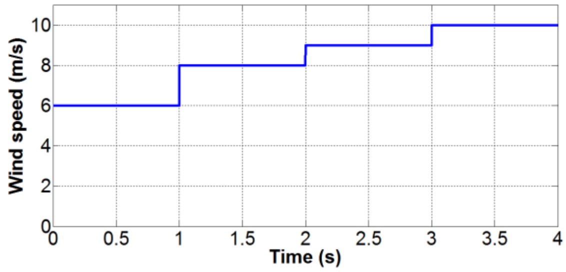

Fig. 4. Wind speed variation

The next figure shows the rotor speed needed to catch the maximum of accessible power produced by the wind turbine. It is easy to remark the coincidence between the blue curve which refers to the actual mechanical speed and the red curve which presents the reference rotor speed.

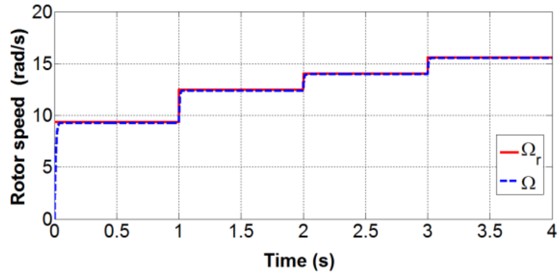

Fig. 5. Rotor speed tracking

Fig.6 and Fig.7 illustrate the control response against instantaneous variation of the stator current references. The quality of reference tracking is justified.

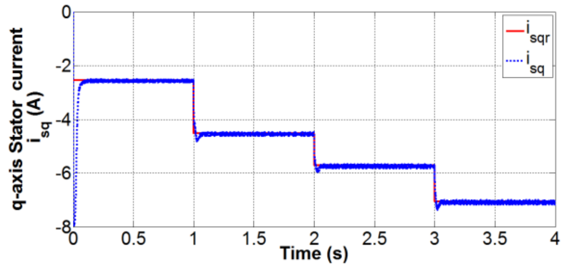

Fig. 6. q- axis stator current tracking

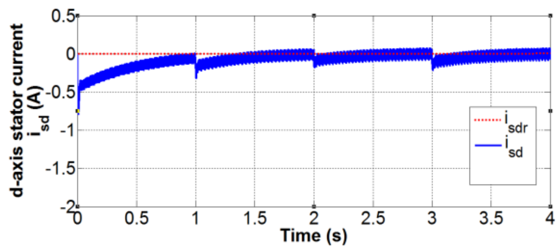

Fig. 7. d- axis stator current tracking

Furthermore, the bus voltage tracking is presented in Fig.8. We can observe that the bus voltage follows the reference trajectory.

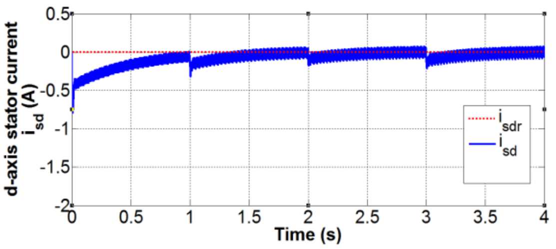

Fig. 8. Bus voltage tracking

The proposed fuzzy controller leads to the MPPT response presented in Fig.9. As illustrated in the figure, the main objective of our MPPT strategy is accomplished. It means that the maximum power point can be quickly achieved despite fast-varying wind velocity.

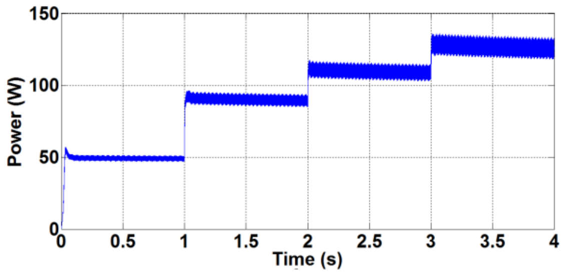

Fig. 9. Wind turbine produced power

In summary, the proposed control topology performance is clearly illustrated by the simulation results.

5. Conclusion

This paper focuses on control strategy dedicated for a wind conversion system with the main objective to ensure maximum peak power tracking (MPPT). The algorithm searches the upper accessible power using a torque reference generated by the wind turbine characteristics. By using robust control based on T-S approach, allowed to track rotational speed, stator current and voltage references which correspond to the optimum power; and therefore operate in the maximum power. So as to preserve good performances and quick response, the controller gains are designed with LMI techniques. Numerical simulations using different measurement of wind speed has validated the proposed control strategy.

As future work, we project to test this control algorithm on the complete structure of WECS as presented in Fig.1.

References

[1] "Time for action: Wind energy in Europe," *European Wind Energy Asso.*,Rome, Italy, Oct. 1991

[2] H. Le-Huy, P. Viarouge, and J. Dickinson, "Application of power electronics in windmill generation systems," *ENERGEX'82 International Energy Conference*, Regina, Canada, pp. 1080–1088, 1982.

[3] T. A. Lipo, "Variable speed generator technology options for wind turbine generators," *NASA Workshop*, Cleveland, OH, May 1984.

[4] H. M. Nguyen and D. Subbaram Naidu, "Advanced control strategies for wind energy systems: an overview," *Proc. of IEEE PES Power Systems Conference and Exposition*, pp. 1-8, Phoenix, AZ, USA, 2011.

[5] M. Mansour , M. N. Mansouri and M. F. Mmımouni, "Study and control of a variable-speed wind-energy system connected to the grid", *International Journal of Renewable Energy Research (IJRER)*, vol. 1, no 2, pp. 96-104, 2011.

[6] M. Kesraoui, N. Korichi, and A. Belkadi, "Maximum power point tracker of wind energy conversion system," *Renewable Energy*, vol. 36, no. 10, pp. 2655-2662, 2011.

[7] H. Li et al., "Development of a unified design, test, and research platform for wind energy systems based on hardware-in-the-loop real time simulation,"*IEEE Trans. on Industrial Electronics*, vol.53, no. 4, pp. 3604-3608, 2006.

[8] A. Meharrar et al., "A variable speed wind generator maximum power tracking based on adaptive neuro-fuzzy inference system," *Expert Systems with Applications*, vol. 38, no. 6, pp. 7659-7664, 2011.

[9] Simoes, M. Godoy, Bimal K. Bose, and Ronald J. Spiegel. "Fuzzy logic based intelligent control of a variable speed cage machine wind generation system." *Power Electronics, IEEE Transactions on*, vol 12, no. 1,pp. 87-95 ,1997.

[10] B. Bahraminejad, Iranpour, M. R., Esfandiari, E, "Pitch Control of Wind Turbines Using IT2FL Controller Versus T1FL Controller", *International Journal of Renewable Energy Research (IJRER)*, vol. 4, no 4, pp. 1077, 2014.

[11] Q. Chen, L. H. Chen, and L. G. Wang, "Wind energy conversion systems using fuzzy sliding mode control," *Proc. of 2011 Chinese Control and Decision Conference*, pp. 1011-1015, Guiyang, China, 2011.

[12] F. Valenciaga and M. R. Puleston, "High-order sliding control of a wind energy conversion system based on a permanent magnet synchronous generator," *IEEE Trans. on Energy Conversion*, vol. 23, no. 3, pp. 860-867, 2008.

[13] D. H. Lee, J. B. Park, and Y. H. Joo, "A new fuzzy Lyapunov function for relaxed stability condition of continuous-time Takagi-Sugeno fuzzy systems," *IEEE Trans. on Fuzzy Systems*, vol. 19, no. 4, pp. 785-791, 2011.

[14] Chian-Song Chiu, Zong-Han Li, and Yi-Huan Chen, "T-S Fuzzy Direct Maximum Power Point Tracking of Wind Energy Conversion Systems, " *International Journal of Fuzzy Systems*, vol. 15, no. 2, June 2013.

[15] A. H. Besheer, H. M. Emara, and M. M. Abdel_Aziz, "Fuzzy based output feedback control for wind energy conversion system: an LMI approach," *Proc. of IEEE Power Systems Conference and Exposition*, pp. 2030-2037, Atlanta, GA, 2006.

[16] M. Narimani and H. K. Lam, "Relaxed LMI-based stability conditions for Takagi-Sugeno fuzzy control systems using regional-membership-functionshape-dependent analysis approach," *IEEE Trans. on Fuzzy Systems*, vol. 17, no. 5, pp. 1221-1228, 2009.

[17] P. Gahinet, A. Nemirovski, A. J. Laub, and M. Chilali, "LMI Control Toolbox,". *Natick, MA: The Math Works* ,1995.

[18] C.Tseng, Bor sen Chen, and Uang H.J., "Fuzzy tracking control design for non linear dynamic system via ts fuzzy model," *IEEE Trans fuzzy system*, vol. 9, pp. 381–392, 2001.

[19] F. Zheng, Q-G. Wang, and T. H. Lee., "Output tracking control of mimo fuzzy nonlinear systems using variable structure control approach," IEEE *Trans. Fuzzy system*, vol.10, no. 6, 2002.

[20] Chong. Lin, Q-G. Wang, and T. H. Lee. "Output tracking control for nonlinear via t-s fuzzy model approach," *IEEE Trans. systems. Cybernetics*, vol. 36, no. 2, 2006.

[21] M. Dahmane, J. Bosche, and A. El-Hajjaji, "Control of Wind Conversion System Used in Autonomous System," *Energy Procedia*, vol. 62, pp. 482-491, 2014.

[22] A. Boyette, "Contrôle-commande d'un générateur asynchrone à double alimentation avec système de stockage pour la production éolienne," *Diss. University of Henri Poincaré-Nancy I*, 2006.

[23] M. M. S., Camara, M. B., Camara, B. Dakyo, and H. Gualous, "Modélisation et commande d'une génératrice synchrone à aimant permanant pour la production et l'injection des énergies offshores dans un réseau," *Symposium de Génie Électrique*, 2014.

[24] H. De Battısta, Mantz, R. J., "Dynamical variable structure controller for power regulation of wind energy conversion systems", *Energy Conversion, IEEE Transactions on*, vol. 19, no. 4, pp. 756-763, 2004.

[25] Z. Qiu, Zhou, K., Li, Y., Yıngtao, "Modeling and control of diode rectifier fed PMSG based wind turbine", *Electric Utility Deregulation and Restructuring and Power Technologies (DRPT),* 4th International Conference on. IEEE, pp. 1384-1388, 2011.

[26] L. Krichen, B. Francois, and A. Ouali, "A fuzzy logic supervisor for active and reactive power control of a fixed speed wind energy conversion system,"*Electric Power Systems Research*, vol .78, no. 3, pp. 418-424, 2008.